

See discussions, stats, and author profiles for this publication at: <https://www.researchgate.net/publication/268485558>

Towards joint use of side scan sonar and subbottom profiler data for the automatic quantification of marine habitats. Case study: Lourdas gulf, Kefalonia isl., Greece.

Conference Paper · June 2014

CITATIONS

2

READS

186

4 authors:



Elias Fakiris

University of Patras

58 PUBLICATIONS 516 CITATIONS

SEE PROFILE



Despina Zoura

University of Leeds

10 PUBLICATIONS 33 CITATIONS

SEE PROFILE



George Ferentinos

University of Patras

146 PUBLICATIONS 3,051 CITATIONS

SEE PROFILE



George Papatheodorou

University of Patras

215 PUBLICATIONS 3,866 CITATIONS

SEE PROFILE

Some of the authors of this publication are also working on these related projects:



Contribution to the study of the Hellenic Karst [View project](#)



SASMAP [View project](#)

TOWARDS JOINT USE OF SIDE SCAN SONAR AND SUB-BOTTOM PROFILER DATA FOR THE AUTOMATIC QUANTIFICATION OF MARINE HABITATS. CASE STUDY: LOURDAS GULF, KEFALONIA ISL., GREECE.

Fakiris Elias^a, Zoura Despina^a, Ferentinos George^a, Papatheodorou George^a

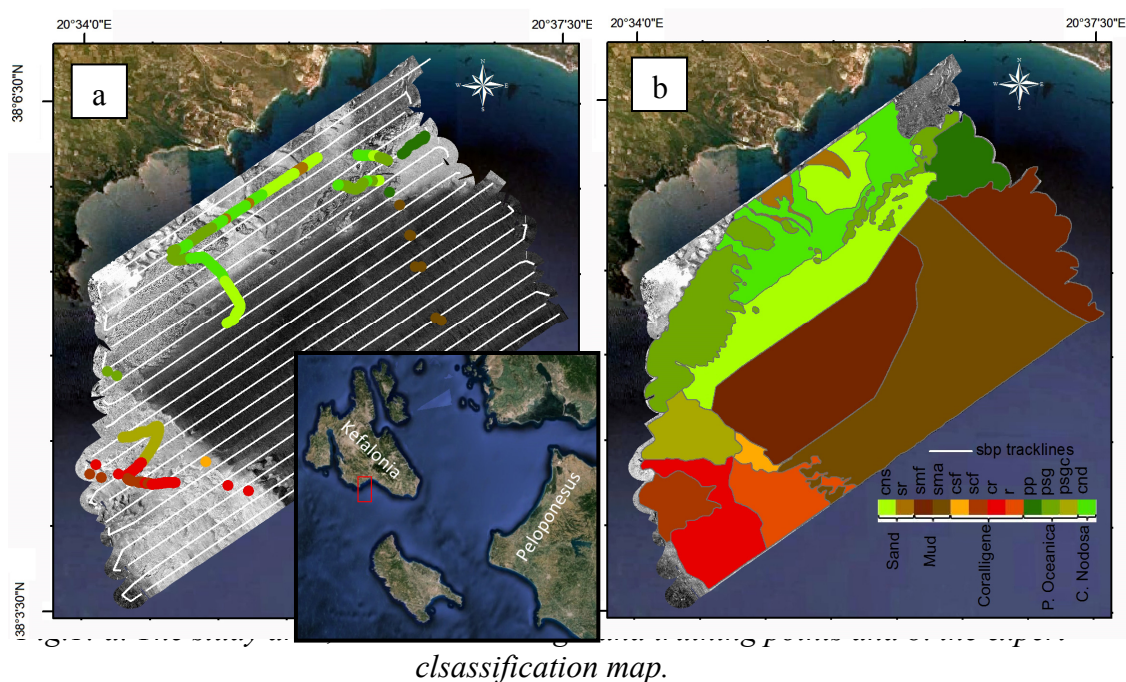
^a Laboratory of Marine Geology and Physical Oceanography, Department of Geology, University of Patras, 265 00 Rion, Greece.

Abstract: *Although Multi-beam Echo Sounder tends to be the preferred tool nowadays towards gaining knowledge about the seafloor, numerous surveys have been and are still being performed by simultaneously using conventional Side-Scan Sonars (SSSs) and Sub-Bottom Profilers (SBPs). This is in respect of gaining fast, wide scale, three dimensional imaging of the seafloor and its substrate, extracting maximum value from a single and time limited survey. The combination of these two systems offer good knowledge of both the stratigraphy and the habitats of the seabed, aspects often linked to each other. However, a basic drawback is the inconsistency between their mapping scales, while SSS produces high resolution backscatter maps (of much higher density than MBES ones) while SBP produces substrata information of high vertical but very low horizontal density. In this work, 100 kHz SSS and 3.5 kHz SBP data, collected simultaneously during a geophysical survey at Lourdas gulf, Kefalonia Island, Greece, underwent post-processing and analysis, to extract numerous statistical features from both the seafloor and its substrate, towards automatic seafloor classification. The SSS records were mosaicked using Geocoder and the mosaic image was subjected to textural analysis, using the SonarClass software tool, to extract a large number of features. Unsupervised classification of the SSS features led to an accurate segmentation of the seafloor into homogenous regions. The SBP images were processed using multi-scale elongated steerable filters, to detect all seismic reflectors, and numerous features were extracted regarding the acoustic transparency and density of the seismic reflectors (layering) as well as the rugosity of the seabed. Supervised classification of the SBP features exhibited their high ability to discriminate between different known sea bed types, making them suitable for use as a substitute of traditional ground discrimination systems. The combination of the SBP track classes to the SSS segmentation, led to a full coverage - high detailed classification map of the study area.*

Keywords: *sidescan sonar, subbottom profiler, acoustic classification, habitat mapping*

1. INTRODUCTION – STUDY AREA

Although Single Beam Echo Sounders (SBES) are traditionally the core for most automatic ground discrimination systems (AGDS), in this work, an effort to validate the high frequency Sub-Bottom Profiling (SBP) systems against revealing useful information about the seabed habitats in an automated way is realized. However, while AGDS use calibrated sounders, SBPs are inherently un-calibrated ones, and thus effort must be put to extract quantitative descriptors that are not significantly affected by variations in system operation setups, such as recording gains and transmitting power. Despite this complication, SBPs are able to reveal much more information about the seabed sediments and habitats than SBES, due to their penetration ability, and so the prospect of implementing a system to automatically quantify and classify SBP data seems appealing.



SBES and SBP methods have a great disadvantage comparing to the swath sonar systems, where data is collected from the most of the seabed, that they need to interpolation between the ship-tracks, thus less rigorously discriminate between defined seabed classes. Yet, information provided by swath and single beam sonar systems regard totally different physical properties of the sea-bed and they both deserve to be accounted to gain better insight into the seafloor processes and habitats. Through SSS images one can delineate and describe the different seabed types and features in terms of their acoustic intensity and texture. On the other hand, high frequency sub-bottom profiling systems offer information about the roughness and the hardness of the seabed, parameters strongly correlated to the sediment type and its vegetation. Concurrent substrata information may be used to quantify the acoustic transparency and layering of the superficial sediments and to detect the possible substrate, which, if it is close to the seafloor, it may influence the seabed biota.

In this work 3,5Khz SBP and 100Khz SSS data, collected simultaneously during a geophysical survey at Lourdai gulf, Kefalonia Island, Greece, are combined to produce full coverage classification maps. Lourdai exhibits a complex seafloor with frequent

changes in sediment and habitat types, making it a really challenging environment for automatic acoustic classification processes. During the coupled SSS - SBP survey, 94.2 km of way-lines have been carried out, insonifying a total area of 16.4 km² (fig.1.a). The validation of the seabed types was realized through a 7.2 km long ground truthing survey using a tow camera, which, in combination to the SSS mosaic and the SBP data, led to an expert manual classification, as shown in fig.1.b, some classes of which can be merged to produce a rougher classification scheme (see legend in fig.1.b). According to the suggested methodological scheme, the SSS mosaic is firstly used to segment the seafloor in large homogenous areas, while descriptors extracted from the SBP records are subjected to supervised classification trained by data samples in proximity to the groundtruthing points. Full coverage classification maps are finally produced by assigning its majority class to each one of the segmented areas.

2. SIDESCAN SONAR MOSAICKING AND SEGMENTATION

Acoustic returns from SSS produce intense geometric and radiometric artefacts in the created backscatter mosaics, which in turn affect the accuracy of facies delineation. Although Geocoder [1] has mainly been designed for use with MBES backscatter data, it can be used as well for raw SSS data, allowing the creation of more visually consistent mosaics. Specifically, application of its advanced AVG, despeckle and blending options led to a drastically improved SSS mosaic in Lourdas Gulf (fig.1.a). Backscatter values from different acquisition lines were reduced to a common scale of scattering strength, while their overlapping areas were blended so that only the best quality data is kept. The above, in conjunction with AVG application, led to a beautified mosaic.

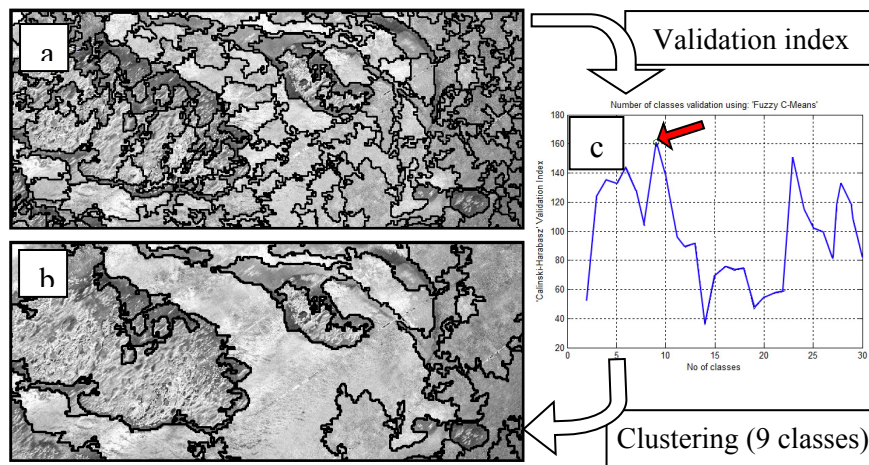


Fig.2: Details from the two SSS segmentation scales: a. EDISON superpixels, b. fuzzy c-means clustering and c. Validation index suggesting 9 classes.

The segmentation of the mosaicked data was performed in two different scales. The first involved fine scale segmentation using the mean shift method (fig.2.a), as implemented in the EDISON software [2]. At this stage, the segmented regions, usually called superpixels, are quite small and so few of them coincide with the SBP way-lines. We need a larger scale segmentation, the separate regions of which will still honour the

exact boundaries of the various sea-bottom types, while most of them will coincide with a considerable number of SBP points. For this, we utilized clustering of the SSS mosaic via textural parameters extracted from 30x30m distinct image patches. Feature extraction and clustering took place through the Matlab tool SonarClass [3]. It employs three feature extraction algorithms, namely first order grey-level statistics, grey level co-occurrence matrices (GLCMs) and 2D power spectrum specifications, constituting feature vectors of totally 11 descriptors. The clustering took place using the fuzzy c-means algorithm and the optimal number of classes was decided upon the Calinski-Harabasz validation index, which clearly suggested 9 classes (fig.2.c). For each superpixel created in the fine scale segmentation stage, the median value from the underlying SonarClass classes was estimated, to produce a higher resolution classification map. This is moreover a noise-free, smoother version of the raw SonarClass classification map due to the local median consideration. What we need at this stage is the separate homogenous areas produced by the clustering process rather than their class assignments. This way the output is a segmentation map rather than a classification one.

3. AUTOMATIC TRACKING OF SEISMIC REFLECTORS

A set of local (pixel wise) contrasts ($c_{w,h,k}$) are defined, each extracted using couples of adjacent rectangular features of width w and height h , rotated at direction k (see fig.1). Filtering the image using such rectangular features of a single direction, results in a directional boundary enhancement filter. In this work, that the enhancement of prolonged seismic reflectors is needed, we set the feature's dimension to a fixed w to h ratio equal to 1:16. Thus, from now on, a certain scale a refers to a feature of dimensions $w=a$ and $h=a/16$ spatial units, giving the $c_{a,k}$ local contrast. Contrasts are further normalized by taking their ratio to their maximum possible value, which normally is the range (R) of data values (e.g. 256 in the case of 8bit images). In this way, local contrast takes values between 0 and 1, with unity implying the maximum contrast possible. According to the above, the normalized local contrast ($C_{a,k}$) for a fixed rotation k and scale a , is defined as:

$$C_{a,k}(x,y) = \frac{|c_{a,k}(x,y)|}{R} \quad (1)$$

Rotation invariant normalized local contrast of a given scale (a) is defined as the average ($\mu_{a,n}$) of local contrast along a set of n directions (eq. 2). This defines a rotational invariant boundary enhancement filter. An additional elementary statistical parameter derived in the context of this work is the standard deviation ($\sigma_{a,n}$) of the contrasts along the n directions (equation 3):

$$\mu_{\alpha,n}(x,y) = \frac{1}{n} \sum_{k=k(1)}^{k(n)} C_{\alpha,k}(x,y), \quad \sigma_{\alpha,n}(x,y) = \sqrt{\frac{1}{n-1} \left[\sum_{k=k(1)}^{k(n)} C_{\alpha,k}(x,y)^2 - \left(\sum_{k=k(1)}^{k(n)} C_{\alpha,k}(x,y) \right)^2 \right]} \quad (2), (3)$$

The above boundary enhancement filters are dependent on the scale under consideration, which can decrease their efficiency against reflectors of different thicknesses. For this, $\mu_{a,n}$ and $\sigma_{a,n}$ are averaged over a number of s successive scales, finally providing rotation and scale invariant boundary enhancement filters $\bar{\mu}_{s,n}$, $\bar{\sigma}_{s,n}$ (eq. 4,5).

Another statistic measure considered, coefficient of variation: $CV_{s,n} = \overline{\sigma}_{s,n} / \overline{\mu}_{s,n}$, proved to be beneficial for the accurate tracking of the seabed (see fig.3).

$$\overline{\mu}_{s,n}(x, y) = \frac{1}{S} \sum_{a=a(1)}^{a(s)} (\mu_{\alpha,n}(x, y)), \quad \overline{\sigma}_{s,n}(x, y) = \frac{1}{S} \sum_{a=a(1)}^{a(s)} \sigma_{\alpha,n}(x, y) \quad (4)$$

In the context of the present work, four feature scales were chosen in a quadratic fashion, namely $a(1-4)=4, 8, 16$ and 32m and four rotations, $k(1-4)=0, 45, 90, 135^\circ$. In order to achieve maximum computational speed, the above filters were implemented using Haar-like features and integral images, as described in [4]. After successively filtering an SBP image, detection of the seismic reflectors was performed by finding the peaks in $\overline{\mu}_{s,n}$ as a function of depth, for equidistant pings. An example of applying boundary enhancement filtering and seismic reflectors detection on a typical SBP image is shown in fig.3.

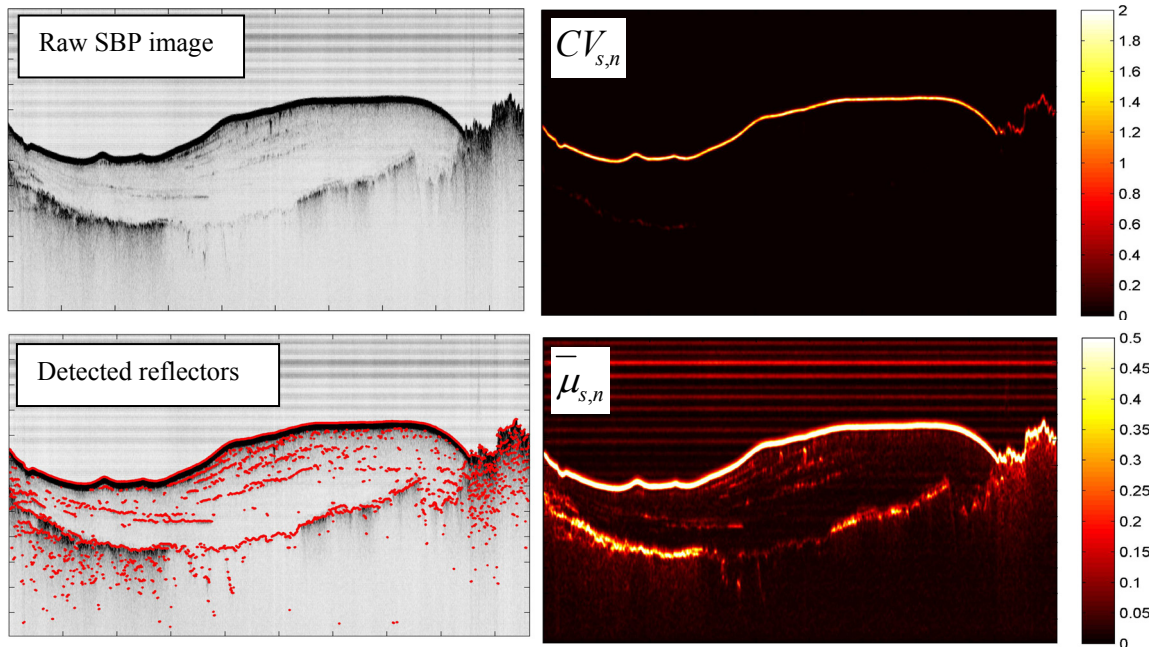


Fig.3: A Raw SBP image, $\overline{\mu}_{s,n}(x, y)$ $CV_{s,n}$ filtering results, and the detected reflectors

4. PARAMETERIZATION OF THE SEISMIC PROFILES

A total number of 28 features have been extracted from equidistant points (pingwise) of the seismic profiles (Table 1). Five of them regard the local bathymetric profile using rugosity and curvative definitions, eighteen use $\overline{\mu}_{s,n}$ to quantify the distinctness and density of the seismic reflectors, three regard simple counting of the tracked reflectors and estimation of the maximum penetration ability into the sediments while finally two features concern the intensity change, in the raw SBP images, in the first few meters below the seafloor. Table 1 gives a short description for each extracted feature.

No	Feature	Description
1	Depth	The depth at each analyzed sample. The seabed tracking was performed using the depth of the first higher peak of $CV_{s,n}$ for the considered ping.
2, 3	Std, Mn	The value of $\overline{\mu}_{s,n}$ and $\overline{\sigma}_{s,n}$ along the tracked seabed.
4 5	Rug50 Rug250	The rugosity defined as the variance of the depth over a window of 50 and 250m respectively, extending both sides the analyzed ping.
6 7	Curv250, Curv500	The local curvature, calculated as $1/r$, where r is the radius of a circle, fitted through least squares at a bathymetric profile 250 and 500m long respectively, extending both sides the analyzed ping.
8	Pen	The distance between the seabed and the deeper tracked seismic reflector.
9	NoR	The number of tracked seismic reflectors under the seabed.
10, 11, 12	StdS, MeanS, CVS	The mean, std and coefficient of variation of the $\overline{\mu}_{s,n}$ within the first 2,5m below the seabed.
13, 14, 15	MeanSR,StdSR, CVSR	The mean, std and coefficient of variation of the $\overline{\mu}_{s,n}$ peak values (tracked seismic reflectors) within the first 2,5m below the seabed.
16	NoSR	The number of tracked seismic reflectors within the first 2,5m below the seabed.
17, 18, 19, 20, 21	CVR, KurtR, StdR, MeanR, SkewR	The mean, std, kurtosis, skewness and coefficient of variation of the $\overline{\mu}_{s,n}$ peak values (tracked reflectors) within the penetration zone (the between the tracked seabed and the deeper tracked reflector).
22, 23, 24, 25, 26	CVP, MeanP, KurtP, StdP, SkewP	The mean, std, kurtosis, skewness and coefficient of variation of the $\overline{\mu}_{s,n}$ within the penetration zone.
27	Ratio	The ratio between the seismic intensity (using the raw image) of the first reflection zone (estimated by <i>Knee</i>) and a 2m thick zone below it.
28	Knee	An estimation of how prolonged (thick) the first seismic reflection (seabed) is. It is calculated by extracting the cumulative sum of the seismic signal at a 2m thick region below the seabed and finding its knee point (where the curve is approximated by a pair of lines).

Table 1: The features extracted from each analyzed (pingwise) sample of the seismic images.

5. RANKING AND VALIDATION OF THE SBP FEATURES TOWARDS SUPERVISED CLASSIFICATION

The value of the designed parameters towards meaningfully quantifying the seabed is validated against their ability to produce accurate classification maps through supervised algorithms. Three classification algorithms, preceded by a feature selection wrapper method, were tested in WEKA software tool [5] against their performance about both the fine classification and the rough (merged classes) classification scheme. Two training sets were used, one consisting of a random 10% of the whole dataset (Exp.10%), labelled according to the expert classification map and another consisting of SBP samples that are in proximity to the groundtruthing points (GT training dataset). The performance of the classifiers was estimated using three different metrics, namely average true positive rate, Kappa statistic and the mean area under the ROC curves.

Classifier	No of Classes	Selected features	Training Set	TP Rate	Kappa statistic	ROC area
Naive Bayes	Fine classes	1,3,4,6,17,19,23,26,27,28 : 10	Exp.10%	0.746	0.6942	0.955
			GT	0.542	0.4552	0.882
	Rough classes	1,2,4,7,17,18,26,27,28 : 9	Exp.10%	0.868	0.8058	0.975
			GT	<u>0.746</u>	<u>0.6322</u>	<u>0.948</u>
Bayes Network	Fine classes	1,2,3,4,5,7,11,12,17,21,23,25,26,27,28 : 15	Exp.10%	0.874	0.8475	0.987
			GT	0.248	0.1705	0.654
	Rough classes	1,2,3,4,7,10,16,20,21,23,24,28 : 11	Exp.10%	0.922	0.886	0.99
			GT	0.342	0.1951	0.685
Decision Tree	Fine classes	1,2,3,5,7,9,15 : 7	Exp.10%	0.86	0.8304	0.944
			GT	0.443	0.3466	0.684
	Rough classes	1,2,7,9,18,21,22,23 : 8	Exp.10%	0.915	0.874	0.964
			GT	0.744	0.6428	0.848

Table 2: The performance of 3 classifiers, validated against two different set of classes (see fig.1.2) and training sets. Exp.10% : training set using the 10% of the whole dataset, GT: training samples collected from SBP points in proximity to the ground truthing.

Naive Bayes classifier, although producing simpler decision boundaries, it outperformed the others when using the more realistic GT training dataset. Although in the ideal case where ground truthing stations are randomly distributed in the study area (Exp.10%), Bayes Network would perform perfectly, it failed in the GT case, probably due to over-fitting bias. The rough classification scheme, seemed to be more easily validated by all classifiers, but the ROC area was significantly high even for the fine classification scheme, when using Naive Bayes. Accordingly, Naive Bayes is considered a good classifier if trained by realistic groundtruthing sample distributions. The later was used to produce the final automatic classification map for our area (fig.4.a). This shows significant similarity to the expert classification map, even though a simple classifier was used, trained only by samples that were close to ground truthing stations.

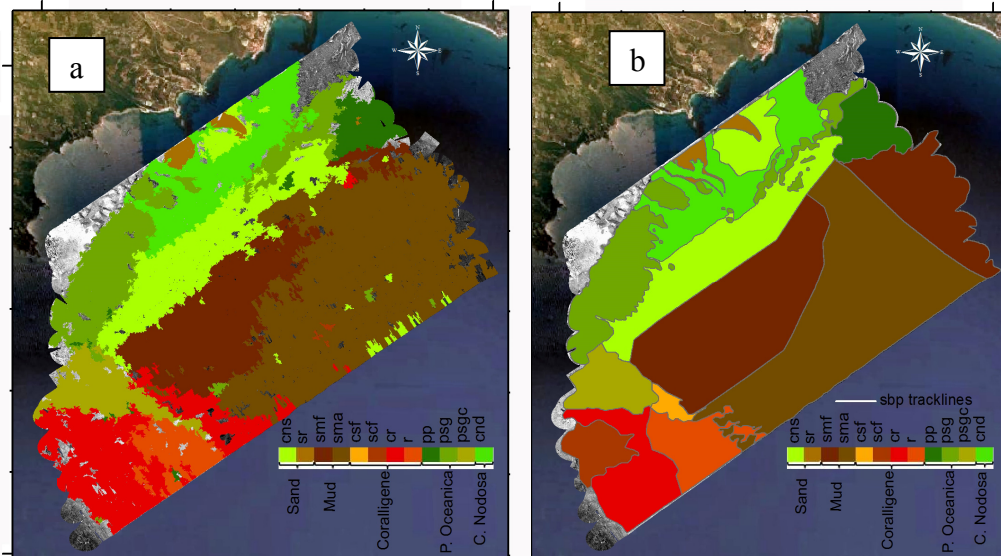


Fig.4: a. The final automatic classification map, produced using Naive Bayes classifier and b. the GT training dataset, compared to the expert manual one.

6. CONCLUSIONS

Through this work it was made evident that high frequency SBP systems, like 3,5 khz pingers and chirps, can be successively used for automatic ground discrimination purposes. The suggested SBP quantification methodology proved to be suitable for supervised classification, indicating that at least some of the extracted features are meaningful. The feature selection stage revealed some certain parameters that seem to have higher discrimination powers. Still, many other parameters played a role in producing more accurate classifications. Finally, using the segmentation of the SSS mosaic led to full coverage, consistent classification maps. In the future it is important to test the suggested method in datasets from other areas to validate its repeatability.

7. ACKNOWLEDGEMENTS

The dataset has been granted by the ETCP “Greece – Italy 2007 – 2013” interdisciplinary Aquaria for the Promotion of Environmental and History. «APREH» program. We thank all the members of the Laboratory of Marine Geology and Physical Oceanography (LMGPO) for the invaluable contribution during the data collection. Finally we thank Ramfos Alexis for kindly providing part of the ground truthing stations.

REFERENCES

- [1] **Rzhanov Y., Fonseca L. & Mayer L**, Construction of seafloor thematic maps from multibeam acoustic backscatter angular response data. *Computers & Geosciences*, 41, pp. 181-187, 2012.
- [2] **Christoudias C., Georgescu B., Meer P.**: Synergism in low-level vision. *16th International Conference on Pattern Recognition*, Quebec City, Canada, vol. IV, 150-155, August 2002.
- [3] **Fakiris, E., Papatheodorou G.**, Sonar Class: A MTALAB toolbox for the classification of side scan sonar imagery, using local textural and reverberational characteristics. In *Proceedings of 3rd International Conference on Underwater acoustic measurements: Technologies & results (eds. Papadakis and Bjorno)*, Nafplion Greece, vol. III, p. 1445-1450, 21st-26th June 2009.
- [4] **Fakiris E., Williams D., Couillard M., Fox W.** Sea-Floor Acoustic Anisotropy and Complexity Assessment Towards Prediction of ATR Performance, in *Proc. International Conference on Underwater Acoustics (UAC)*, Corfu Isl., Greece, 23 - 28 June 2013.
- [5] **Hall M., Frank E., Holmes G., Pfahringer B., Reutemann P., I.H. Witten**, *The WEKA Data Mining Software: An Update*, SIGKDD Explorations, Volume 11, Issue 1, 2009.